AMERICAN JOURNAL OF DIAGNOSTIC IMAGING, 2021
VOL 7, NO. 2
10.5455/ajdi.20201011125201

ORIGINAL ARTICLE

Open Access

Differentiating COVID-19 from swine flu pneumonia on HRCT chest

Somali Ghosh, Nilu Malpani Dhoot, Usha Goenka, Surabhi Jajodia, Sumit Datta
Apollo Gleneagles Hospital, Kolkata, India

ABSTRACT

Objectives: To find features differentiating the coronavirus disease 2019 (COVID-19) from swine flu on high-resolution computed tomography (HRCT).

Methods: A total of 148 COVID-19 patients and 84 swine flu patients were enrolled in the study with positive reverse transcriptase polymerase chain reaction. HRCT lung of these patients from January 2019 to May 2020 were retrospectively analyzed. Findings like ground-glass opacities, consolidation, distribution of lesions, vessel engorgement, reverse halo sign, centrilobular nodules, pleural effusion, and mediastinal lymphadenopathy were evaluated and compared.

Results: Ground-glass opacities in a peripheral distribution, vessel engorgement, and architectural distortion were the predominant findings in COVID-19 pneumonia and showed statistical difference ($p < 0.00001$). Although consolidation was a common finding in both COVID-19 and swine flu, the distribution of these lesions was random in swine flu. Centrilobular nodules and pleural effusion were characteristic findings of H1N1 infection with a statistical difference ($p < 0.00001$). Although reverse halo was found only in COVID-19, it was not statistically significant ($p > 0.01$)

Conclusion: COVID-19 and swine flu, the two viral types of pneumonia that caused pandemics, can be distinguished on HRCT lungs by the presence of lesions typical to each virus infection and the difference in the distribution pattern of the lesions common in both diseases.

ARTICLE HISTORY

Received October 11, 2020
Accepted April 09, 2021
Published September 05, 2021

KEYWORDS

COVID-19; Swine flu, CT, chest, findings

Introduction

In December 2019, in Wuhan, China, a new respiratory infection emerged with clinical features of viral pneumonia [1], which was traced to a new strain of coronavirus, called SARS-COV-2, which originated from bats. It is an RNA virus, and the mode of human-to-human transmission was through droplets and fomites [2]. The high adequate reproduction number (R0) of this virus was 6–6.6 (compared to 1.5 of seasonal flu), which was responsible for its exponential growth, high infectivity, and quick spread [3].

The coronavirus disease 2019 (COVID-19) was declared a pandemic on March 11, 2020, by the World Health Organization. The total number of confirmed cases till May 2020 was 5.59 million, and the total number of deaths was 350k**.** Males above the age of 60 years were more affected than females [4]. The principal diagnostic test for COVID-19 is a real-time reverse transcriptase polymerase chain reaction (RT-PCR) [5].

The swine influenza (H1N1) first emerged in human beings in Mexico in mid-April 2009 [6]. This swine-origin virus caused respiratory infections ranging from mild to severe illness [7] and was initially called the H1N1pdm09 virus. Children and young people were more affected as they had low immunity. About one-third of the people above the age of 60 years had antibodies, most likely because they had previous exposure to some older strains of the H1N1 virus [8]. The number of deaths worldwide in the first year of the pandemic, 2009–10, was between 151,700 and 575,400 [9]. Since then, the infection by this virus became seasonal, mostly emerging in the winter months.

Significant outbreaks by the H1N1 virus occurred in 2015 and 2017, with 38,811 confirmed cases and 22,66 deaths in 2017 [10]. H1N1 influenza is

Contact Nilu Malpani Dhoot ✉ drniludhoot@gmail.com Apollo Gleneagles Hospital, Kolkata, India.

© 2021 The Authors. This is an open access article under the terms of the Creative Commons Attribution NonCommercial ShareAlike 4.0 (https://creativecommons.org/licenses/by-nc-sa/4.0/).

associated with the highest mortality compared to other influenza viruses. The confirmatory laboratory test for swine flu is RT-PCR [11]. The sensitivity of swine flu RT-PCR is 90%–95% [12]. Since both COVID-19 and H1N1 influenza viruses have a common zoonotic origin, it is expected that COVID-19 is also likely to be endemic and show seasonality, just like the influenza virus.

High-resolution computed tomography (HRCT) is a powerful tool for the early diagnosis of COVID-19 and swine flu pneumonia. It is also the best method to define the extent of pulmonary involvement, detect associated complications and superadded infections, and in the follow-up of patients showing failure to respond to conventional treatment [13]. There are chest findings that are specific for viral pneumonia. Our study aimed to see if we could differentiate the two types of viral pneumonia, COVID-19 and swine flu, by HRCT chest.

Method and Material

This retrospective study was approved by our institutional research committee. We analyzed the HRCT scans of 148 patients with COVID-19 and 84 cases of swine flu from our database from January 2019 to May 2020, of which the COVID-19 cases were more recent from March to May 2020. All the selected cases were RT-PCR positive for the respective viruses. Eleven cases in which HRCT showed other interstitial lung diseases and malignancy were excluded from the study. Six of these were COVID-19 patients and five of them were of swine influenza.

HRCT image acquisition

Low-dose HRCT chest scans for COVID-19 patients were carried out in a dedicated scanner using Aquilion Prime 160 CT system (Toshiba, Tokyo, Japan) helical mode scanner. The tube voltage was 120 kvp and the tube current was set to a low dose of 50 mAs. Low-dose CT was used to reduce the radiation dose to the patients. The images were taken from the level of the thyroid gland to the level of the pancreas, in full inspiration whenever possible. Slice thickness was 0.8 mm. Images were reconstructed in the bony algorithm, and both the mediastinal window (window width 450 HU, level 35HU) and lung window (window width 1,500 HU, level 500–700 HU) were studied. Multiplanar reformation of axial images in coronal and sagittal planes was carried out and interpreted whenever necessary. The swine flu cases were imaged in Philips Brilliance 16 CT system (Philips, Amsterdam, Netherlands). These images were taken with a tube voltage of 120 kvp and 100 mAs. Two radiologists with an experience of more than 5 years interpreted the HRCT scans in consensus after resolving any difference in opinion through discussion.

The CT images were evaluated for airspace opacification, ground-glass opacity (GGO), and/or consolidation, with regard to their presence, distribution pattern (peripheral, central, or both), lobes predominantly involved (upper, middle, or lower lobes), and the shape of GGO (rounded or diffuse). The presence of reticulation, crazy paving pattern, vascular dilatation, reverse halo sign, subpleural curvilinear lines, subpleural bands, and architectural distortion were also recorded. In addition, other findings like pleural effusion, mediastinal lymphadenopathy, air bronchogram, centrilobular nodules, tree-in-bud sign, bronchial wall thickening, airspace nodules, and air trapping were also noted.

Consolidation was defined as a homogeneous increase in pulmonary parenchymal attenuation that obscures the margins of vessels and airway walls, with/without an air bronchogram. GGO indicated a hazy increase in attenuation of the lung, but with preservation of bronchial and vascular margins. The crazy paving pattern was defined as GGO with an interlobular or intralobular septal thickening. Vascular dilatation was taken as a vessel diameter more than 3 mm. The reverse halo sign was described as a focal GGO surrounded by consolidation. Fibrosis and subpleural fibrotic strands were noted as architectural distortions and subpleural bands. Centrilobular nodules were small nodules in the center of the secondary pulmonary lobule. The tree-in-bud sign was a nodular dilatation of centrilobular branching structures that resemble a budding tree and represent exudative bronchiolar dilatation [14].

Descriptive statistical analysis was carried out to calculate the means with corresponding standard deviations (SD). Chi-square test was carried out to find the associations. $p < 0.05$ was taken to be statistically significant.

Results

Demographics

The mean age (mean ± SD) of the COVID-19 patients was 46.26 ± 18.83 years, with a range of 15–85 years, and the median age was 45 years. Most of the patients (54.9%) were in the age group between 20 and 49 years. Male to female ratio (M:F) was 1.5:1.0,

with 59.9% of the patients were male and 40.1% were female.

The mean age (mean ± S.D.) of the H1N1 patients was 57.726 ± 14.03 years with a range of 18–83 years, and the median age was 59 years. Most of the patients (54.9%) were in the age group between 35 and 69 years with a male to female ratio of 0.6:1.0. 38.0% were male, while 62.0% were female. Table 1 shows the age distribution of patients with COVID-19 and H1N1.

The *t*-test showed that the mean age of the patients infected with H1N1 was significantly more than that of the patients with COVID-19 (t_{219} = 5.12; $p < 0.0001$).

Table 2 shows the sex distribution of patients with COVID-19 and H1N1 in our cohort. Males were infected more by COVID-19, whereas females were infected more with H1N1 in our study group.

CT analysis

Table 3 shows the various morphological CT findings in COVID-19 pneumonia and H1N1 pneumonia (Fig 1, 2).

Airspace opacification (GGO and/or consolidation) was present in 100% of COVID-19 patients, while they were observed in only 54 out of 79 (68.4%) H1N1 patients. Thirty-four patients with swine flu (43.0%) had consolidation predominance compared to 12 patients of COVID-19 group (8.4%). GGO was more common than consolidation in COVID-19 and was seen in 100% of the patients, and consolidation was more common than GGO in H1N1 infection. While the reverse halo sign was seen in 7% of COVID-19 patients, it was conspicuously absent in swine flu patients. The centrilobular nodule was a typical feature in H1N1 infection. Nine swine flu patients (11.4%) had centrilobular nodules as the only finding in the chest. Vessel engorgement and architectural distortion were frequently observed in COVID-19 patients and rarely found in H1N1 disease; this difference was statistically significant. Pleural effusion and mediastinal lymphadenopathy were found far more frequently in H1N1 when compared to COVID-19.

Bilateral involvement was more common than unilateral involvement in both diseases. Peripheral distribution and lower lobe predominance were noted in COVID-19 pneumonia (88%), while both peripheral and central distribution and diffuse lung involvement were more characteristically observed in H1N1 (68%). Additionally, pericardial effusion was present in three patients, cavity in one patient, and cystic bronchiectasis in one patient with H1N1 infection. Whether bronchiectasis was due to the disease itself or was pre-existing could not be ascertained. None of these findings were seen in the COVID-19 group.

Table 1. Age distribution of the patients.

Descriptive statistics age (in years)	COVID (*n* = 142)	H1N1 (*n* = 79)	*t*-test (t_{219})	*p*-value
Mean ± SD	46.26 ± 18.83	57.72 ± 14.03	5.12	<0.0001 S
Median	45	59		
Range	15–85	18–83		

Table 2. Gender distribution of patients.

Gender	COVID (*n* = 142)	H1N1 (*n* = 79)
Male	85 (59.9%)	30 (38.0%)
Female	57 (40.1%)	49 (62.0%)
Total	142 (100%)	79 (100%)

Discussion

Both swine flu and COVID-19 have caused pandemics and mainly affect the respiratory system. Since 2015, H1N1 has been causing seasonal outbreaks. We expect COVID-19 will soon become an endemic disease and will have a seasonal recurrence. In this retrospective study, we have defined

Table 3. CT imaging findings in COVID-19 and H1N1 infections.

CT Findings	COVID-19 (*n* = 142)	H1N1 (*n* = 79)	*p*-value
GGO	142 (100%)	36 (45.5%)	$p < 0.00001$
Consolidation	102 (71.8.%)	45 (56.9%)	$p < 0.05$
Vessel engorgement	126 (88.7%)	4 (5%)	$p < 0.00001$
Architectural distortion	56 (39.4%)	1 (1.2%)	$p < 0.00001$
Centrilobular nodules	0 (0.0%)	55 (69%)	$p < 0.00001$
Pleural effusion	5 (3.5%)	21 (26.5%)	$p < 0.00001$
Mediastinal lymphadenopathy	1 (0.7%)	6 (7.5%)	$p < 0.05$
Reverse halo sign	10 (7.0%)	0 (0.0%)	$p < 0.05$

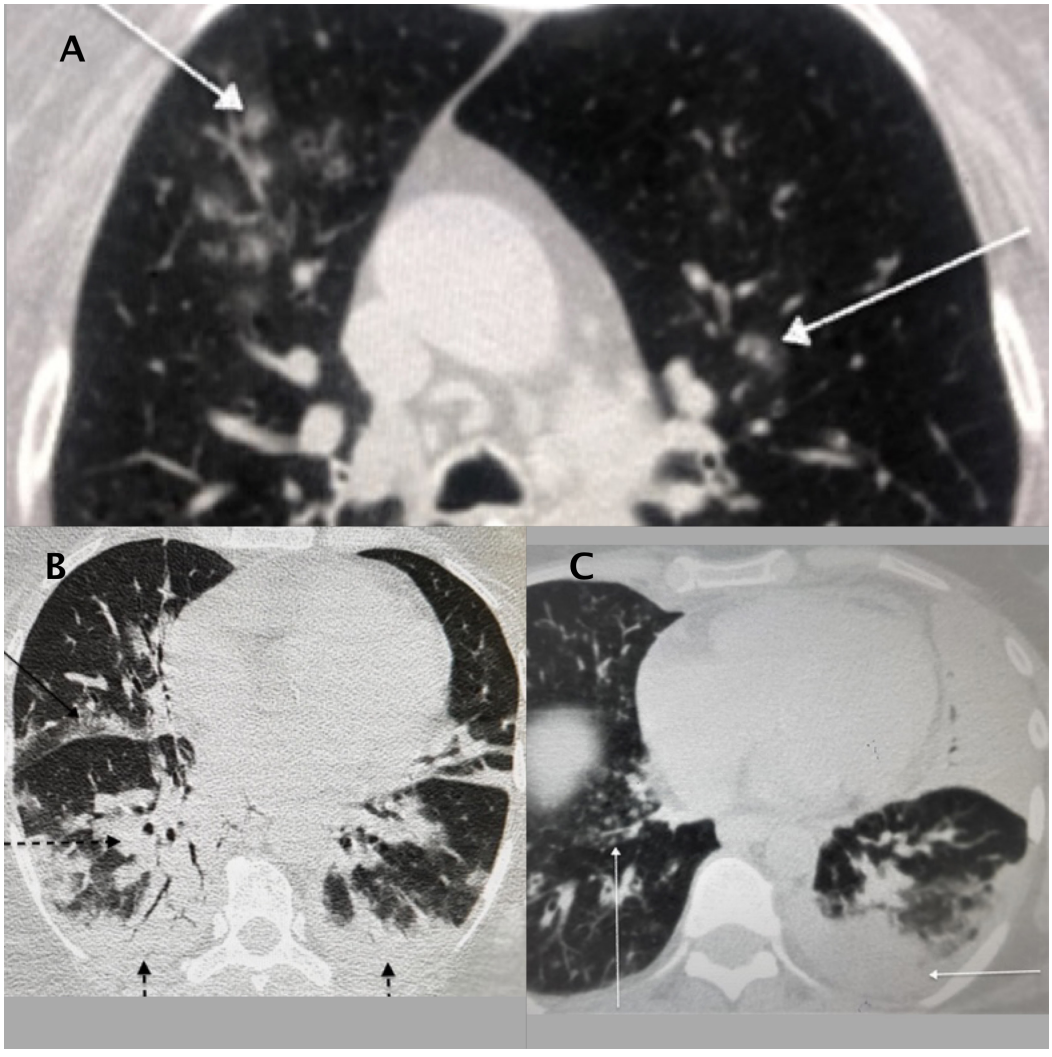


Figure 1. Findings in swine flu, HRCT lung window, axial section. (A) Multiple centrilobular nodules marked by arrows. (B) Consolidation is marked by dotted arrows and ground-glass opacities are marked by solid arrows. (C) Left-sided pleural effusion is marked by the horizontal arrow and centrilobular nodules are marked by the vertical arrow.

the CT features of infections caused by both these viruses and differentiated the two infections based on HRCT findings.

COVID-19 and swine pneumonia commonly present with fever, cough, and shortness of breath. The diseases have similar clinical features and differentiating them clinically can be challenging. Non-productive cough, fatigue, and gastrointestinal symptoms were more pronounced in COVID-19 compared to swine flu [15]. Elevation of C-reactive protein and a decrease in eosinophil count was more common in COVID-19 [16]. RT-PCR assay, because of its high specificity, is the principal method for detecting COVID-19 [17]. However, the sensitivity of RT-PCR for COVID-19 is lower and is around 60%–70% [18]. Causes for false-negative results are defective kits, insufficient organisms due to inappropriate collection, less viral load, etc. [19].

Chest CT showed typical imaging findings despite the negative PCR in many patients of COVID-19 [20]. Compared to RT-PCR, the sensitivity of chest CT in COVID-19 was much higher, reaching up to 97% [21]. Hence, HRCT chest plays a vital role in the early diagnosis of COVID-19 disease [18]. We believe it is essential to differentiate the chest CT findings in COVID-19 from those in H1N1 infection because of the clinical overlap and because the COVID-19 infection may coexist in the community with H1N1 infection, which has shown seasonal outbreaks following the pandemic in 2009.

The mean age of patients for swine flu was higher than COVID-19 patients (57.7±14 years compared to 46.26±18 years) in our study. There was a male preponderance in COVID-19 patients, with 59.9% male. Similar results were obtained in a study from China on 507 COVID-19 patients, where the

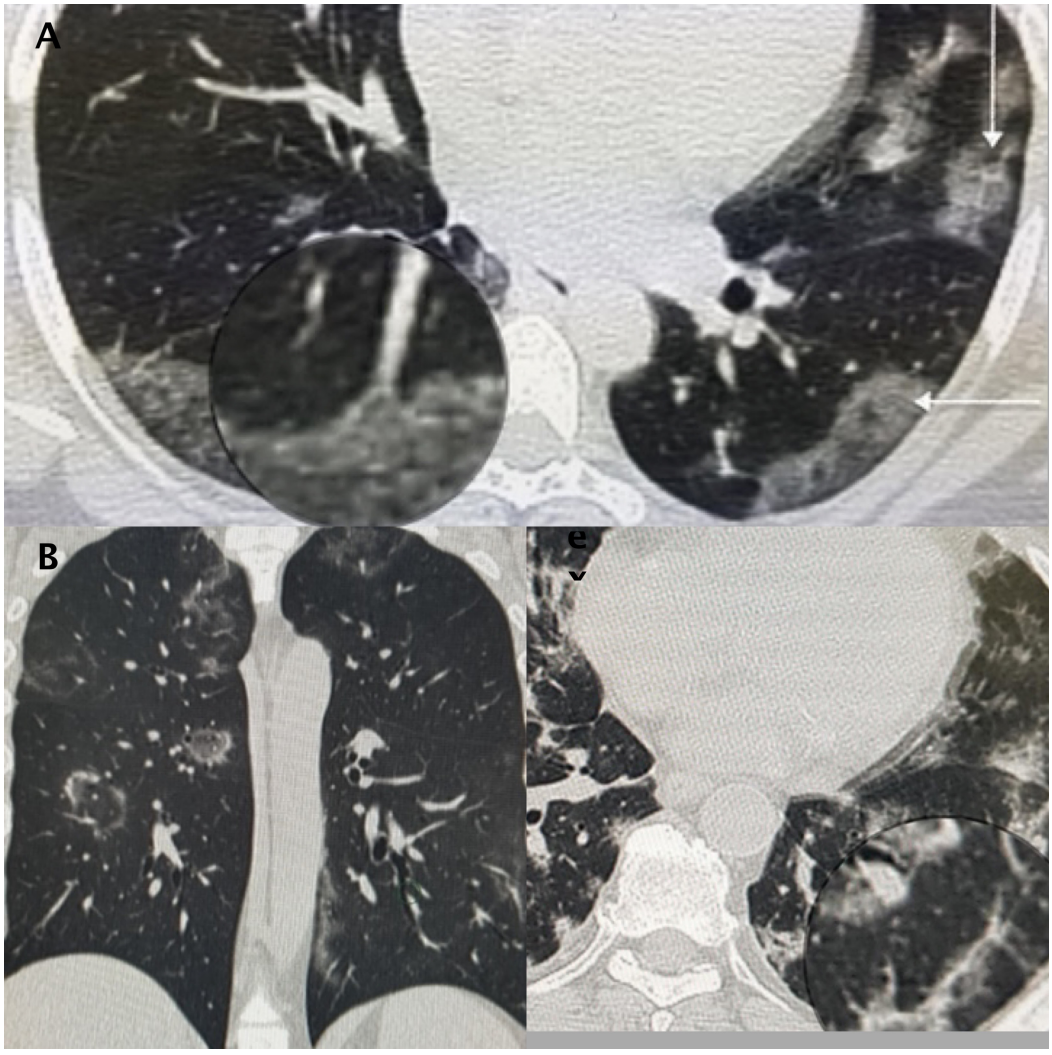


Figure 2. Findings in COVID-19, HRCT lung window (A) Axial section shows peripheral GGO and vessel engorgement in the magnified section. (B) Coronal section shows reverse halo. (C) Axial section shows architectural distortion in magnified view.

mean age was 47 years, of which 55% were male [22]. A study on 39 patients by Göya et al. [24] also showed a higher mean age of H1N1 patients, which was 53.9±14 years [24]. However, most previous studies on H1N1 showed a predominantly younger cohort to be affected, as in a study from Rajasthan, India, where the mean age was 37.09±16.07 years [23]. Females were more likely to develop severe H1N1 disease requiring hospitalization, as shown by a study from the USA, where 53.2% of females require hospitalization against 46.8% of males [25]. A higher incidence of female involvement was also seen in our study of 79 inpatients of H1N1, in which 49 (69%) patients were females.

Although GGO is a common finding in both COVID-19 and swine flu infections, it is far more common in COVID-19. We found GGOs in 100% of COVID-19 cases, compared to 36% of the cases in a swine flu infection. A study in China showed that GGO was present in 100% of COVID-19 cases, with peripheral distribution in 93.6% [26]. In our study, peripheral distribution was seen in 88% of the cases. Consolidation was present in 71.8% of COVID-19 patients and 56.9% of swine flu patients in our study. In some studies, H1N1 patients showed GGO in up to 74.5% of the cases, and consolidation was present in 72.6% of the patients [24]. Although airspace opacities were the predominant finding in both COVID-19 and swine flu, the distribution of these opacities was random in H1N1 patients [27], as in our study.

Centrilobular nodules were the hallmark findings for H1N1 in our study seen in 69% of the cases. In a study in Brazil with a cohort of 40%, 40% of H1N1 patients showed centrilobular nodules [28], while these nodules were not seen in any of the

COVID-19 cases. A similar experience has been seen in a study differentiating COVID-19 from other pneumonia [29].

Vessel engorgement is probably due to abnormal vasoregulation, microvascular thrombosis, and intrapulmonary shunting [30]. It is a common finding seen in 88% of our COVID-19 patients and was also shown to be present in 85% in another study on 48 COVID-19 patients [27]. Vessel engorgement, however, was found in only 5% of swine flu patients in our study, making it an important differentiating feature between the two infections.

A well-documented finding in COVID-19 was the reverse halo sign seen in 4% of the cases in a study by Bernheim et al. [31]. It was also seen in 7% of our patients but not seen at all in H1N1 patients. Architectural distortion was seen in a study by Lomoro et al. [32] in 28.6% of the patients of COVID-19 [32], and it was seen in 56% of patients in our study. Fibrosis in H1N1 develops later in the disease, which is not seen at all in our study. The mean time of fibrosis was observed as 22.7 ± 15.8 days in a study by Li et al. [33]. In all our patients, CT scan was carried out at admission, and none of them showed fibrosis as the scan was carried out very early in the course of the disease.

About 18% of the H1N1 patients showed pleural effusion [34], and it was also seen in 21% of the patients in our study. Pleural effusion was significantly less in COVID-19 patients in our study (5%). It was found in 13% of a study cohort of 81 COVID-19 patients by Shi et al. [35]. Mediastinal lymphadenopathy was present in 0.7% of our COVID-19 patients. It is not a typical feature in COVID-19 patients, and a similar experience was reported in a study by Guan et al. [26]. Mediastinal lymphadenopathy, however, is common in swine flu patients, and was present in 7.5% of swine flu patients in our study. It was seen in 16.1% of swine flu pneumonia patients in a study by Bakhshayeshkaram et al. [36]. There is a scoring system for COVID-19 pneumonia which predicts the prognosis of the disease [37]; however, there is no such system in the swine flu disease.

CT is known to have a high sensitivity, but the specificity is known to be low in the diagnosis of viral pneumonia. It is as low as 25%–33%, as reported in this study [38].

A moderate-sized patient study group could be a limitation of our study. Secondly, in our study, the duration of symptoms after which the CT was carried out was not taken into account for both the viruses.

To conclude, alveolar opacities were the most common findings in both swine flu and COVID-19 patients. GGOs were much more common in COVID-19 compared to swine flu, and the distribution in COVID-19 was peripheral compared to a random location in swine flu patients. While reverse halo sign was found characteristically in COVID-19 patients, centrilobular nodules were an exclusive finding in swine flu patients. Vessel engorgement was much more frequent in COVID-19, whereas pleural effusion and mediastinal lymphadenopathy were more common in swine flu. These characteristic findings in HRCT lung can, therefore, help the radiologists to differentiate COVID-19 from swine flu.

References

[1] Huang C, Wang Y, Li X, Ren L, Zhao J, Hu Y, et al. Clinical features of patients infected with 2019 novel coronavirus in Wuhan, China. Lancet 2020; 395(10223):497–506.

[2] Charlton CL, Babady E, Ginocchio CC, Hatchette TF, Jerris RC, Li Y, et al. Practical guidance for clinical microbiology laboratories: viruses causing acute respiratory tract infections. American Society for Microbiology. Clin Microbiol Rev 2018; 32(1):1–47.

[3] Ridenhour B, Kowalik JM, Shay DK. Unraveling R0: considerations for public health applications. Am J Public Health 2014; 104(2):e32–41.

[4] Yi Y, Lagniton PNP, Ye S, Li E, Xu RH. COVID-19: what has been learned and to be learned about the novel coronavirus disease. Int J Biol Sci 2020; 16(10):1753–66.

[5] Ai T, Yang Z, Hou H, Zhan C, Chen C, Lv W, et al. Correlation of chest CT and RT-PCR testing for coronavirus disease 2019 (COVID-19) in China: a report of 1014 cases. Radiology 2020; 296(2):E32–40.

[6] Gibbs AJ, Armstrong JS, Downie JC. From where did the 2009 'swine-origin' influenza a virus (H1N1) emerge? Virol J 2009; 6:207.

[7] Novel Swine-Origin Influenza A (H1N1) Virus Investigation Team, Dawood FS, Jain S, Finelli L, Shaw MW, Lindstrom S, et al. Emergence of a novel swine-origin influenza A (H1N1) virus in humans. N Engl J Med 2009; 360(25):2605–15.

[8] Baldo V, Bertoncello C, Cocchio S, Fonzo M, Pillon P, Buja A, et al. The new pandemic influenza A/(H1N1)pdm09 virus: is it really "new"? J Prev Med Hyg 2016; 57(1):E19–22.

[9] The 2009 H1N1 pandemic: summary highlights, April 2009-April 2010. Center for disease control, Atlanta, GA, 2010.

[10] Kulkarni SV, Narain JP, Gupta S, Dhariwal AC, Singh SK, Macintyre CR. Influenza A (H1N1) in India: Changing epidemiology and its implications. Natl Med J India 2019; 32(2):107–8.

[11] Chauhan C, Narang J, Pundir S, Singh S, Pundir CS. Laboratory diagnosis of Swine flu: a review. Artif Cells Nanomedicine Biotechnol 2013; 41(3):189–95.
[12] Ginocchio CC, McAdam AJ. Current best practices for respiratory virus testing. J Microbiol 2020; 74(1):93–8.
[13] Amorim VB, Rodrigues RS, Barreto MM, Zanetti G, Hochhegger B, Marchiori E. Influenza A (H1N1) pneumonia: HRCT findings. J Bras Pneumol 2013; 39(3):323–9; doi:10.1590/S1806-37132013000300009
[14] Hansell DM, Bankier AA, MacMahon H, McLoud TC, Müller NL, Remy J. Fleischner society: glossary of terms for thoracic imaging. Radiology 2008; 246(3):697–722.
[15] Tang X, Du RH, Wang R, Cao TZ, Guan LL, Yang CQ, et al. Comparison of hospitalized patients with ARDS caused by COVID-19 and H1N1. Chest 2020; 158(1):195–205.
[16] Li Q, Ding X, Xia G, Chen HG, Chen F, Geng Z, et al. Eosinopenia and elevated C-reactive protein facilitate triage of COVID-19 patients in fever clinic: a retrospective case-control study. EClinicalMedicine 2020; 23:100375.
[17] Zitek T. The appropriate use of testing for COVID-19. West J Emerg Med 2020; 21(3):470–2.
[18] Fang Y, Zhang H, Xie J, Lin M, Ying L, Pang P, et al. Sensitivity of chest CT for COVID-19: comparison to RT-PCR. Radiology 2020; 296(2):E115–7.
[19] Tahamtan A, Ardebili A. Real-time RT-PCR in COVID-19 detection: issues affecting the results. Expert Rev Mol Diagn 2020; 20(5):453–4.
[20] Hao W, Li M. Clinical diagnostic value of CT imaging in COVID-19 with multiple negative RT-PCR testing. Travel Med Infect Dis 2020; 34:101627.
[21] Hong KH, Lee SW, Kim TS, Huh HJ, Lee J, Kim SY, et al. Guidelines for laboratory diagnosis of coronavirus disease 2019 (COVID-19) in Korea. Ann Lab Med 2020; 40(5):351–60.
[22] Sun K, Chen J, Viboud C. Early epidemiological analysis of the coronavirus disease 2019 outbreak based on crowdsourced data: a population-level observational study. Lancet Digit Health 2020; 2(4):e201–8.
[23] Kumar S. A study of outbreak of Swine Flu (H1N1) in North - West Zone of Rajasthan (current status - 2015). J Assoc Physicians India 2016; 64(7):46–9. PMID: 27759342.
[24] Göya C, Yavuz A, Hamidi C, Güli M. The role of initial radiologic and clinical manifestations in predicting the prognosis for pneumonia caused by H1N1 influenza. J Thorac Dis 2014; 6(6):752–9.
[25] Klein SL, Pekosz A, Passaretti C, Anker M, Olukoya P. Sex, gender and influenza in achieving gender equality and health equity. World Health Organization Geneva, Geneva, Switzerland, 2010; pp 1–62.
[26] Guan CS, Lv ZB, Yan S, Du YN, Chen H, Wei LG, et al. Imaging features of coronavirus disease 2019 (COVID-19): evaluation on thin-section CT. Acad Radiol 2020; 27(5):609–13.
[27] Amorim VB, Rodrigues RS, Barreto MM. Influenza A (H1N1) pneumonia: HRCT findings. J Bras Pneumol 2013; 39(3):323–9.
[28] Amorim VB, Rodrigues RS, Barreto MM. Computed tomography findings in patients with H1N1 influenza A infection. Radiol Bras 2013; 46(5):299–306.
[29] Luo L, Luo Z, Jia Y, Zhou C, He J, Lyu J, et al. CT differential diagnosis of COVID-19 and non-COVID-19 in symptomatic suspects: a practical scoring method. BMC Pulm Med 2020; 20:1–9.
[30] Lang M, Som A, Carey D, Reid N, Mendoza DP, Flores EJ, et al. Pulmonary vascular manifestations of COVID-19 pneumonia. Radiol Cardiothorac Imaging 2020; 2(3):1–26.
[31] Bernheim A, Mei X, Huang M, Yang Y, Fayad ZA, Diao NZK et al. Chest CT findings in Coronavirus disease-19 (COVID-19): relationship to duration of infection. Radiology 2020; 295:685–91.
[32] Lomoro P, Verde F, Zerboni F, Simonetti I, Borghi C, Fachinetti C, et al. COVID-19 pneumonia manifestations at the admission on chest ultrasound, radiographs, and CT: single-center study and comprehensive radiologic literature review. Eur J Radiol Open 2020; 7:100231.
[33] Li P, Zhang JF, Xia XD, Su DJ, Liu BL, Zhao DL, et al. Serial evaluation of high-resolution CT findings in patients with pneumonia in novel swine-origin influenza - A (H1N1) virus infection. Br J Radiol 2012; 85(1014):729–35.
[34] Schoen K, Horvat N, Guerreiro NFC, de Castro I, de Giassi KS. Spectrum of clinical and radiographic findings in patients with diagnosis of H1N1 and correlation with clinical severity. BMC Infect Dis 2019; 19(1):1–8.
[35] Shi H, Han X, Jiang N, Cao Y, Alwalid O, Gu J, et al. Radiological findings from 81 patients with COVID-19 pneumonia in Wuhan, China: a descriptive study. Lancet Infect Dis 2020;20(4):425–34.
[36] Bakhshayeshkaram M, Saidi B, Tabarsi P, Zahirifard S, Ghofrani M. Imaging findings in patients with H1N1 influenza a infection. Iran J Radiol 2011; 8(4):230–4.
[37] Dhoot NM, Goenka U, Ghosh S, Jajodia S, Chand R, Majumdar S, et al. Assigning computed tomography involvement score in COVID-19 patients: prognosis prediction and impact on management. BJR Open 2020; 2:20200024.
[38] Xu B, Xing Y, Peng J, Zheng Z, Tang W, Sun Y, et al. Chest CT for detecting COVID-19: a systematic review and meta-analysis of diagnostic accuracy. Eur Radiol 2020; 30(10):5720–7.